

Integrating peatlands and permafrost into a dynamic global vegetation model:

2. Evaluation and sensitivity of vegetation and carbon cycle processes

R. Wania,^{1,2} I. Ross,^{3,4} and I. C. Prentice⁵

Received 25 October 2008; revised 3 April 2009; accepted 7 May 2009; published 22 August 2009.

[1] Peatlands and permafrost are important components of the carbon cycle in the northern high latitudes. The inclusion of these components into a dynamic global vegetation model required changes to physical land surface routines, the addition of two new peatland-specific plant functional types, incorporation of an inundation stress mechanism, and deceleration of decomposition under inundation. The new model, LPJ-WHy v1.2, was used to simulate net ecosystem production (NEP), net primary production (NPP), heterotrophic respiration (HR), and soil carbon content. Annual peatland NEP matches observations even though the seasonal amplitude is overestimated. This overestimation is caused by excessive NPP values, probably due to the lack of nitrogen or phosphorus limitation in LPJ-WHy. Introduction of permafrost reduces circumpolar (45–90°N) NEP from 1.65 to 0.96 Pg C a⁻¹ and leads to an increase in soil carbon content of almost 40 Pg C; adding peatlands doubles this soil carbon increase. Peatland soil carbon content and hence HR depend on model spin-up duration and are crucial for simulating NEP. These results highlight the need for a regional peatland age map to help determine spin-up times. A sensitivity experiment revealed that under future climate conditions, NPP may rise more rapidly than HR resulting in increases in NEP.

Citation: Wania, R., I. Ross, and I. C. Prentice (2009), Integrating peatlands and permafrost into a dynamic global vegetation model: 2. Evaluation and sensitivity of vegetation and carbon cycle processes, *Global Biogeochem. Cycles*, 23, GB3015, doi:10.1029/2008GB003413.

1. Introduction

[2] Peatlands represent an important ecosystem that has so far not been considered in dynamic global vegetation models (DGVMs). Peatlands are an important component of the Earth system because they accumulate carbon over long timescales [Gorham, 1991; Maltby and Immirzi, 1993; Davidson and Janssens, 2006] and they release methane, which contributes significantly to the global greenhouse effect [Denman *et al.*, 2007]. Peatlands have been omitted from DGVMs, not because of a lack of importance, but because they constitute a very different ecosystem to all others: transitional between terrestrial and aquatic. Plants growing in permanently inundated conditions have to cope with different stress factors compared to terrestrial plants [Cronk and Fennessy, 2001; Pezeshki, 2001; Baird and

Wilby, 1999]. Permanent inundation slows decomposition processes [Freeman *et al.*, 2001] and promotes the accumulation of carbon in the soil, i.e., peat growth [Clymo *et al.*, 1998].

[3] DGVMs are used not only for present-day carbon cycle studies, but also to study future ecosystem changes and climate feedbacks [Sitch *et al.*, 2008]. It is likely that northern regions, where most peatlands are found at present, will experience the fastest rise in temperature over the course of this century [Christensen *et al.*, 2007; Meehl *et al.*, 2007b]. This region coincides with the region where almost all low-altitude permafrost is found. Freezing of soil is an important feature that should be included in DGVMs, as it determines the availability of liquid water and therefore productivity [Beer *et al.*, 2007]. This is true for peatlands and nonpeatlands alike. Permafrost areas show slower rates of peatland carbon accumulation than nonpermafrost areas [Bridgman *et al.*, 2006; Robinson and Moore, 2000], although this difference could be caused by soil temperature and not by the presence of permafrost per se.

[4] This paper evaluates the vegetation dynamics simulated by a widely used vegetation model, the Lund-Potsdam-Jena DGVM (LPJ) [Sitch *et al.*, 2003; Gerten *et al.*, 2004], modified to include peatlands and permafrost dynamics as new components [Wania *et al.*, 2009]. The main changes to the vegetation dynamics are the

¹Department of Earth Sciences, University of Bristol, Bristol, UK.

²Now at School of Earth and Ocean Sciences, University of Victoria, Victoria, British Columbia, Canada.

³School of Geographical Sciences, University of Bristol, Bristol, UK.

⁴Now at Mathematics and Statistics, University of Victoria, Victoria, British Columbia, Canada.

⁵QUEST, Department of Earth Sciences, University of Bristol, Bristol, UK.

introduction of *Sphagnum* mosses and flood-tolerant C₃ graminoids as new plant functional types (PFTs) and the representation of inundation stress, root exudation, and reduced decomposition under anaerobic conditions. Physical land surface processes, governing soil temperature, water table position, active layer depth, and permafrost distribution were described and evaluated in part 1 [Wania *et al.*, 2009]. Here we examine the effect of the new components on net primary production (NPP), heterotrophic respiration (HR), net ecosystem production NEP = NPP – HR [Chapin *et al.*, 2006], and soil carbon dynamics.

2. Model Description

[5] The model we use here is based on the Lund-Potsdam-Jena dynamic global vegetation model version 1.2 [Sitch *et al.*, 2003; Gerten *et al.*, 2004]. A summary of modifications and a detailed description of changes we have made to the physical land surface processes in the model can be found in part 1 [Wania *et al.*, 2009].

2.1. Peatland Plant Functional Types

[6] We added two new PFTs to LPJ, flood-tolerant C₃ graminoids (e.g., *Carex* spp., *Eriophorum* spp., *Juncus* spp., *Typha* spp.), and *Sphagnum* (Table S1).¹ In the model, these new PFTs occur only on peatlands; we therefore refer to them as “peatland” PFTs. Flood-tolerant C₃ graminoids are adapted to inundation through the presence of aerenchyma, gas-filled root, stem and leaf tissue through which oxygen is transported downward to the root system. In this way the plants avoid anoxia, which would otherwise lead to accumulation of toxic substances in the roots [Wheeler, 1999]. Aerenchymatous plants are important for peatland greenhouse gas emissions because a large proportion of the methane emitted to the atmosphere in wetlands is transported via aerenchyma [Frenzel and Rudolph, 1998; Colmer, 2003; Evans, 2003].

[7] Our parameterization of *Sphagnum* mosses follows Yurova *et al.* [2007] with one exception: at high *Sphagnum* water content, moss photosynthetic activity is not limited by moss water content. Instead, photosynthesis can operate at full capacity at high water contents. The reason for this difference is as follows. At least some *Sphagnum* spp. require high pore water CO₂ concentrations for growth; if such high pore water CO₂ concentrations are provided, the plants grow well in water [Smolders *et al.*, 2001]. Most studies showing an apparent decline of photosynthesis at high water content have been conducted using deionized water [Silvola and Aaltonen, 1984; Silvola, 1991; Williams and Flanagan, 1996; Titus *et al.*, 1983], which either has very low concentrations of dissolved CO₂ or is CO₂-free. However, the natural environment for *Sphagnum* is highly acidic [Clymo, 1984a] with dissolved CO₂ concentrations of up to a few mmol L⁻¹ [Roelofs *et al.*, 1984; Smolders *et al.*, 2001], favorable to *Sphagnum* growth.

[8] Under the assumption that *Sphagnum* mosses can assimilate dissolved CO₂ from pore water, we adjust the CO₂ concentration available to the *Sphagnum* PFT. We use

a mean pore water CO₂ concentration, χ_p , of 934 $\mu\text{mol L}^{-1}$ [Smolders *et al.*, 2001] and assume that the CO₂ concentration near the surface of the peat, χ_{acro} , is either the pore water concentration, if the water table is at the surface, or a linear mixture between the pore water concentration and the atmospheric CO₂ concentration, χ_a :

$$\chi_{\text{acro}} = \min\left(\chi_p, \chi_p + (\chi_p - \chi_a) \frac{\langle \text{WTP} \rangle}{z}\right), \quad (1)$$

where z is depth in the soil column and $\langle \text{WTP} \rangle$ is the annual mean water table position. (Note that rainwater was not considered to be an important source of CO₂ for *Sphagnum* mosses.) This approach captures the observation that CO₂ concentrations above peat hummocks are elevated (personal observations by L.P.M. Lamers cited by Lamers *et al.* [1999]) and hence are likely to represent a mixture of atmospheric CO₂ and CO₂ released from peat pore spaces. In our model photosynthesis calculations, χ_{acro} replaces the atmospheric CO₂ concentration for *Sphagnum*.

[9] *Sphagnum* photosynthesis has been shown to decrease when moss water content decreases [Silvola, 1991; Williams and Flanagan, 1996, 1998]. Here we use water table position as a surrogate for moss water content [Clymo and Hayward, 1982], and we reduce moss gross primary production as a function of water table position. A daily moss photosynthesis capacity, cap_{moss} , is set by

$$\text{cap}_{\text{moss}} = \begin{cases} 1, & \text{WTP} > -150 \\ 1 - (-\text{WTP} - 150) a_{\text{cap}}, & -280 < \text{WTP} \leq -150 \\ 0.3, & \text{WTP} \leq -280 \end{cases} \quad (2)$$

where $a_{\text{cap}} = (1 - 0.3)/(-150 + 280)$. The numerical values in equation (2) were chosen so that full growth is maintained down to a water table level of –150 mm (loosely on the basis of Clymo and Hayward [1982]), while a linear decrease in moss productivity is prescribed for WTP < –150 mm. (Different species of *Sphagnum* show different WTP thresholds below which desiccation sets in; that is, hummock species tolerate low water contents better than lawn species, so that only a coarse approximation is possible in a global modeling context.) The lower water table position limit in LPJ-WHY of –300 mm does not lead to complete desiccation of mosses. A complete cessation of moss photosynthetic activity therefore does not occur.

[10] A growth restriction was also applied to flood-tolerant C₃ graminoids. This PFT is typical in peatlands with a constantly high water table. Field experiments have shown that graminoid production increases when WTP rises and decreases when WTP falls [Thormann *et al.*, 1998]. When the water table position falls below –100 mm, we therefore reduce this PFT’s monthly gross primary production, GPP_m (g C m⁻²) depending on mean monthly water table position (WTP_m):

$$\text{GPP}_m \longrightarrow \text{GPP}_m + \text{GPP}_m (\text{WTP}_m + 100)/200, \quad (3)$$

$$\text{WTP}_m < -100.$$

¹Auxiliary materials are available in the HTML. doi:10.1029/2008GB003413.

[11] The water table position, WTP_m (mm) is negative when below the surface so that the term $(WTP_m + 100)/200$ will be negative and result in a reduction of GPP_m .

2.2. Inundation Stress

[12] Flooding of vegetated areas leads to anoxic conditions in the rooting zone, causing accumulation of ethylene within plants and lowered redox potentials which lead to the accumulation of phytotoxins, impeding plant growth [Wheeler, 1999; Pezeshki, 2001]. If not adapted to inundation stress, plants die within a few days under such conditions [Wheeler, 1999; Larcher, 2003]. Each plant functional type in LPJ-WHY is assigned a water table threshold above which they experience inundation stress. Monthly gross primary production is reduced by a monthly inundation stress factor which depends on the number of days the plant functional type has experienced stress and a parameter measuring the maximal survivable duration of inundation, which counts how many days per month a plant functional type can survive under inundation (Table S1).

2.3. Decomposition Rates Under Inundation

[13] Decomposition rates in LPJ-WHY are estimated by

$$k = k_{10} R_T R_{\text{moist}}, \quad (4)$$

where k is the actual decomposition rate and k_{10} is the decomposition rate at 10°C (for exudates, litter, and the slow and intermediate carbon pool). R_T is the temperature response function according to Lloyd and Taylor [1994] and Sitch et al. [2003]. For nonpeatland grid points, R_{moist} increases with increasing soil moisture w

$$R_{\text{moist}} = \frac{1 - e^{-w}}{1 - e^{-1}}, \quad (5)$$

reaching its maximum at the water holding capacity. In peatlands, however, the water holding capacity is exceeded as the soil floods. Decomposition rates under anaerobic conditions are slow because anoxia limits phenol oxidase activity and causes phenolic compounds to accumulate [Freeman et al., 2001]. Phenolic compounds suppress the activity of hydrolase, a pivotal enzyme for the degradation of organic material [Freeman et al., 2001]. Ratios of observed aerobic to anaerobic CO_2 production, $r_{\text{aer:anaer}}$, range from 1.4–2.7 [Segers, 1998]. We therefore calculate the moisture response as

$$R_{\text{moist}} = 1/r_{\text{aer:anaer}}, \quad (6)$$

giving values for R_{moist} of 0.37–0.71. After some experimentation and examination of the resulting decomposition rates, we chose a value of R_{moist} of 0.35 to be used in equation (4) for peatland grid cells.

2.4. Litter Accumulation

[14] Litter in LPJ is accumulated at the end of the year and added to the litter pool all at once in January. This scheme can result in decreasing decomposition over the year as less litter becomes available in later months. To

avoid this effect, the annual freshly accumulated litter in LPJ-WHY is split evenly between all months, and after each month, one twelfth of the newly accumulated litter is added to the existing litter pool. This modification leads to a more homogeneous decomposition rate over the year.

2.5. Soil Carbon Storage

[15] In LPJ, decomposed litter is split into a fraction that goes directly to the atmosphere as heterotrophic respiration and a fraction that goes into soil carbon storage. The soil carbon pool consists of an intermediate and a slow carbon pool with turnover times of 33.3 and 1000 years, respectively, at 10°C [Sitch et al., 2003]. These turnover times are weighted by functions of soil temperature and soil moisture (equation (4)).

[16] The peat column may be separated into the acrotelm and the catotelm [Ingram, 1983]. The main distinction between the two is that the catotelm has constant water content whereas the acrotelm has a fluctuating water content. One consequence of this difference is that the catotelm experiences continuously anaerobic conditions while the acrotelm has periodically aerobic conditions. Decomposition is thus much slower in the catotelm. Peat is partially decomposed organic material produced by the vegetation on top of the acrotelm and slowly pushed downward as more material accumulates. In steady state, the acrotelm maintains its depth [Clymo et al., 1998]. Once peat is below the minimum water table position and is therefore continuously inundated, it becomes part of the catotelm. In order to mimic the carbon transfer from the acrotelm to the catotelm, we assume that the intermediate carbon pool in LPJ-WHY represents the acrotelm and the slow pool the catotelm. In LPJ-WHY, carbon is transferred from the acrotelm (intermediate carbon pool) to the catotelm (slow carbon pool) at a rate of $12 \text{ g m}^{-2} \text{ a}^{-1}$ [Clymo, 1984b]. This transfer begins only once the acrotelm has reached a carbon content of 7.5 kg C m^{-2} , which constitutes a fully developed acrotelm. The threshold of 7.5 kg C m^{-2} is based on the assumptions that the acrotelm is 0.3 m thick and the bulk density of the acrotelm is 50 kg m^{-3} [Clymo and Hayward, 1982; Clymo, 1984b], corresponding to about 25 kg C m^{-3} if we assume that 50% of dry matter is carbon (approximately as given by Gorham [1991] and Clymo et al. [1998]).

[17] In addition to this new carbon transfer from the acrotelm to the catotelm, we maintain the carbon input to the slow carbon pool from litter accumulation in LPJ, which in “reality” may correspond to decaying roots. The majority of accumulating, nondecomposing litter goes into the intermediate soil carbon pool; only 1.5% goes into the slow carbon pool.

2.6. Root Exudates

[18] Root exudates are critical for methane production [Chanton et al., 1995; Ström et al., 2005; Christensen et al., 2003] and also important for the terrestrial carbon cycle as, on average, 15–20% of photosynthesized carbon is exuded by plant roots [Whipps and Lynch, 1983; Helal and Sauerbeck, 1984; Hütsch et al., 2002]. We set the fraction of NPP produced as root exudates to 17.5% and subtract this from monthly NPP. The exudates pool has a fast turnover rate, $k_{10}^{(\text{exu})}$,

Table 1. Net Ecosystem Exchange Values (Eddy Covariance Technique) Reported in the Literature^a

Site	Coordinates		Type	Time Period	Mean	Range	Reference
Bakchar bog, WSL, Russia	56.85°N	82.97°E	bog	1999	-108		<i>Friborg et al.</i> [2003]
Churchill, Canada	58.75°N	94.07°W	fen	1997–1999	-28	-55/-10	<i>Laflour et al.</i> [2001]
Degerö, Sweden ^b	64.18°N	19.55°E	mixed acid mire	2001–2002	-55	-61/-48	<i>Sagerfors et al.</i> [2008]
Faejemyr, Sweden	56.25°N	13.55°E	temperate, eccentric bog	2005–2006	-22	±5.4	<i>Lund et al.</i> [2007]
FCRN tower, Alberta, Canada	54.82°N	113.52°W	rich fen	2004	-144	±32	<i>Syed et al.</i> [2006]
Kaamanen, Finland ^b	69.13°N	27.28°E	subarctic fen	1997–2002	-22	-56/-1	<i>Aurela et al.</i> [2004]
Mer Bleue, Canada ^c	45.4°N	75.5°W	raised ombrotrophic bog	1999	-60		<i>Moore et al.</i> [2002]
Mer Bleue, Canada ^b	45.4°N	75.5°W	raised ombrotrophic bog	1998–2004	-40	-110/0	<i>Roulet et al.</i> [2007]
SW Ireland	51.92°N	9.92°W	blanket bog	2003–2004	-55	-61/-49	<i>Sottocornola and Kiely</i> [2005]
Average ± S.D.					-59.3 ± 41.4		

^aValues in parentheses indicate the length of measurement in days. All data are given as $\text{g C m}^{-2} \text{a}^{-1}$.

^bSite used for seasonal NEP comparison.

^cChamber measurements only.

in the range of 1–2 weeks at 10°C. Its overall decomposition rate follows equation (4). Even though methane emissions are not considered in this current manuscript, we wanted to mention the inclusion of root exudates in LPJ-WHy since carbon allocated to root exudates will cause a minor temporal shift of heterotrophic respiration.

2.7. Leaf Dark Respiration

[19] We use a single calculation method for the leaf dark respiration R_{leaf} throughout the model:

$$R_{\text{leaf}} = bV_{\text{max}}, \quad (7)$$

where V_{max} is the maximum rate of CO_2 uptake and b is a scaling factor set to 0.015, 0.02, and 0.03 for C_3 plants, C_4 plants [Haxeltine and Prentice, 1996; Sitch et al., 2003], and mosses [Yurova et al., 2007], respectively.

3. Data and Experiments

[20] Here we describe data and experiments briefly and refer the reader to part 1 [Wania et al., 2009] for a detailed description. LPJ-WHy reads in a soil type classification for each grid cell based on FAO data [Zobler, 1986; FAO, 1991; Sitch et al., 2003] overlain by organic soil carbon data from the IGBP-DIS map [Global Soil Data Task Group, 2000]. Climate data to drive LPJ-WHy were taken from the Climate Research Unit time series data CRU TS 2.1 [New et al., 1999; Mitchell and Jones, 2005]. This data set provides monthly air temperature, cloud cover, total precipitation, and number of wet days for the time period 1901–2002. Atmospheric CO_2 concentrations for 1901–2002 were taken from Etheridge et al. [1996] and Keeling and Whorf [2005]. The first 10 years of the CRU data were repeated 100 times to give 1000 years of model spin-up. This ensures that carbon stocks for nonpeatlands are in equilibrium before the model is driven with the data from 1901–2002 (transient run). Carbon stocks in peatlands do not reach equilibrium in 1000 years of spin-up time, as discussed in section 4.4. During spin-up only, we include an extra 0.5 mm d^{-1} run-on forcing for peatland sites to avoid large vegetation fluctuations caused by climatic oscillations.

[21] Observations of net ecosystem production (NEP) were collected from sites where monthly data were available

for a period greater than 1 year before 2003. We chose Degerö in Sweden, Kaamanen in Finland, Mer Bleue in Canada, and Zotino in Russia (Table 1). The free software package R version 2.5.1 was used for statistical analyses [R Development Core Team, 2008]. Future projections by the ECHAM5 GCM were obtained from the World Climate Research Programme's (WCRP's) Coupled Model Intercomparison Project phase 3 (CMIP3) multimodel ensemble [Meehl et al., 2007a]. The sensitivity experiment was run under CO_2 concentrations of 380 ppmv and 780 ppmv.

4. Results and Discussion

[22] As DGVMs are principally designed for application at the regional to global scale [Smith et al., 2001; Thonicke et al., 2001; Sitch et al., 2003; Gerten et al., 2004], we focus on testing the regional performance of LPJ-WHy. In particular, we concentrate on the evaluation, seasonality, and sensitivity of NEP. We note that the only way to determine if an ecosystem has a positive or a negative land-to-atmosphere carbon exchange is by including all of the carbon species involved in the exchange, i.e., carbon monoxide, methane, dissolved organic and inorganic carbon, volatile organic compounds, and lateral transfer of particulate carbon [Chapin et al., 2006]. Chapin et al. refer to the sum of all of these fluxes as Net Ecosystem Carbon Balance (NECB). Ideally, to simulate the terrestrial carbon balance a model would take account of all of these fluxes. Methane flux has been included into a later version of LPJ-WHy [Wania, 2007], and work to include isoprene

Table 2. Summary of Simulated Net Primary Production, Heterotrophic Respiration, and Net Ecosystem Production for the Gerten Version of LPJ, LPJ-WHy Without Peatlands, and LPJ-WHy With Peatlands Weighted by Fractional Peatland Cover in Each Grid Cell^a

Model Version	NPP	HR	NEP	Soil C
Gerten	17.06	15.41	1.65	891
LPJ-WHy	16.76	15.80	0.96	930
LPJ-WHy peat	16.22	15.18	1.04	968

^aFlux values are mean values over 1991–2000 measured in Pg C a^{-1} . Soil carbon content (Soil C) of the intermediate and slow carbon pools is given as Pg C .

Table 3. Correlation of Monthly Modeled Versus Observed NEP^a

Site	Equation	Pearson's r	p
Degerö	$O = 5.06264 + 0.25882 M$	0.78	<0.001
Kaamanen	$O = -0.0855 + 0.27403 M$	0.77	<0.05
Zotino	$O = 0.79806 + 0.29014 M$	0.85	<0.001
Mer Bleue	$O = 5.3029 + 0.1789 M$	0.41	<0.01

^aM, monthly modeled NEP; O, observed NEP.

into the model is underway (P. N. Foster, personal communication, 2008), but we are still far from being able to simulate NECB comprehensively. Here we focus exclusively on CO₂ exchange.

4.1. Effects of Spin-up Procedures

[23] Peatland formation requires inundation, either caused by stagnation of water, flooding rivers, or terrestrialization of shallow water bodies and lakes [Wieder, 2006]. To reflect these conditions, in peatland grid cells, LPJ-WHY considers the catotelm to be continuously inundated from the beginning. For the acrotelm, however, there are two possibilities. One can begin the simulation with either a water-filled acrotelm or an empty acrotelm. We use an initially empty acrotelm. This slightly unrealistic initial condition and the necessary, but again unrealistic, model spin-up procedure causes problems at some sites, problems that are alleviated by the application of an extra, artificial source of water during the spin-up period only. This additional source of water can be thought of as a run-on term. The difference in water table positions due to this artificial run-on can be seen in Figure S1. (Results from the transient run are not affected.) Figure S2 shows how the added run-on affects NPP of the peatland-specific PFTs at two sites described in part 1 [Wania et al., 2009]. At Salmisuo, run-on during spin-up affects NPP during spin-up, but not later. At BOREAS, on the other hand, flood-tolerant C₃ graminoids do not grow when no run-on is added during spin-up, and this problem seems to persist into the transient period (Figure S2), although total NPP is not significantly affected. NEP shows no significant effect of spin-up method on the transient period (not shown).

4.2. Net Primary Production

[24] Distributions of simulated NPP values for flood-tolerant C₃ graminoids and *Sphagnum* mosses in circumpolar regions are highly skewed. The flood-tolerant C₃ graminoids have a modeled median NPP value close to zero, but a mean value of 97 g C m⁻² a⁻¹. Modeled *Sphagnum* NPP values are similarly skewed, but with a mean of 159 g C m⁻² a⁻¹. Nungesser [2003] summarized NPP values for ten *Sphagnum* species. Our mean value of 159 g C m⁻² a⁻¹ (i.e., 378 g dry matter m⁻² a⁻¹) lies at the upper end of the range of these values, but is not outside the observed range. The majority of peatlands in our study show a modeled NPP of <600 g C m⁻² a⁻¹, but higher values are found in Great Britain and Ireland.

[25] A histogram of modeled NPP values shows one peak at 0–20 g C m⁻² a⁻¹ and a second peak at 200–220 g C m⁻² a⁻¹ for both PFTs (not shown). The peak close to zero can be explained by the absence of vegetation in many grid cells in the far north characterized by constantly

low water table positions and harsh climatic conditions. Combined NPP for flood-tolerant C₃ graminoids and *Sphagnum* shows a peak at zero, a second peak at 180–200 g C m⁻² a⁻¹ and a plateau from 320–460 g C m⁻² a⁻¹. Observations of NPP for three microsites at Mer Bleue, Canada, gave average aboveground NPP values of 140–170 g dry matter m⁻² a⁻¹ for vascular plants in a poor fen and a bog [Moore et al., 2002]. Moore et al. estimated *Sphagnum* NPP as between 140 and 225 g dry matter m⁻² a⁻¹ and total aboveground NPP as between 290 and 360 g dry matter m⁻² a⁻¹. Assuming a carbon content of 50%, we obtain a range of 145–180 g C m⁻² a⁻¹ for total aboveground NPP. Wieder [2006] indicated that total aboveground NPP for North American boreal and sub-boreal bogs and fens were 462 and 319 g dry matter m⁻² a⁻¹, respectively, i.e., approximately 231 and 160 g C m⁻² a⁻¹, only slightly higher than Moore et al.'s estimates. LPJ-WHY produces larger numbers but includes belowground NPP; as Moore et al. [2002] found, belowground biomass in peatlands is typically 4 times as large as aboveground biomass. How this ratio translates to an aboveground-belowground NPP ratio depends on the relative turnover times of aboveground and belowground biomass.

[26] Despite this observation, it remains possible that the model overestimates NPP. Photosynthesis rates in peatlands typically do not reach their theoretical optima for the prevailing light intensity and water availability [Arneeth et al., 2006], perhaps because nitrogen or phosphorus limitation or accumulation of phytotoxins [Pezeshki, 2001; Cronk and Fennessy, 2001] may limit photosynthetic capacity. Bog and fen species from a study site in Maryland, United States, showed lower leaf nitrogen concentrations than terrestrial plants of the same group [Aerts et al., 1999], pointing to a potentially decreased Rubisco concentration, which could be parameterized in the model following the approach by St-Hilaire et al. [2008]. Xu-Ri and Prentice [2008] showed that consideration of the effect of nitrogen uptake on the carbon cycle helped to bring modeled forest NPP in boreal regions closer to observations. In peatlands, where water is abundant but nitrogen is often in short supply [e.g., Malmer and Wallen, 2005; Bragazza et al., 2003, 2005], it may similarly be worthwhile to include nitrogen limitation in order to better simulate NPP (for comparison, see Stöckli et al. [2008]).

4.3. Net Ecosystem Production

4.3.1. Regional NEP Estimates

[27] Figure 1 shows NEP for the circumpolar region north of 45°N for four different model configurations. “LPJ Gerten” (Figure 1a) refers to the Gerten et al. [2004] version of LPJ on which we based our model development. The Gerten et al. model does not include peatlands or permafrost. Figure 1b shows the effect of including permafrost. Decreases in NEP are observed throughout Siberia and in northern Canada and Alaska. The decreases in central and eastern Siberia are mainly due to a reduction in NPP of boreal summergreen needleleaf trees (i.e., *Larix* spp.). This change can be explained by reductions in soil water availability when soil water is allowed to freeze [Beer et al., 2007].

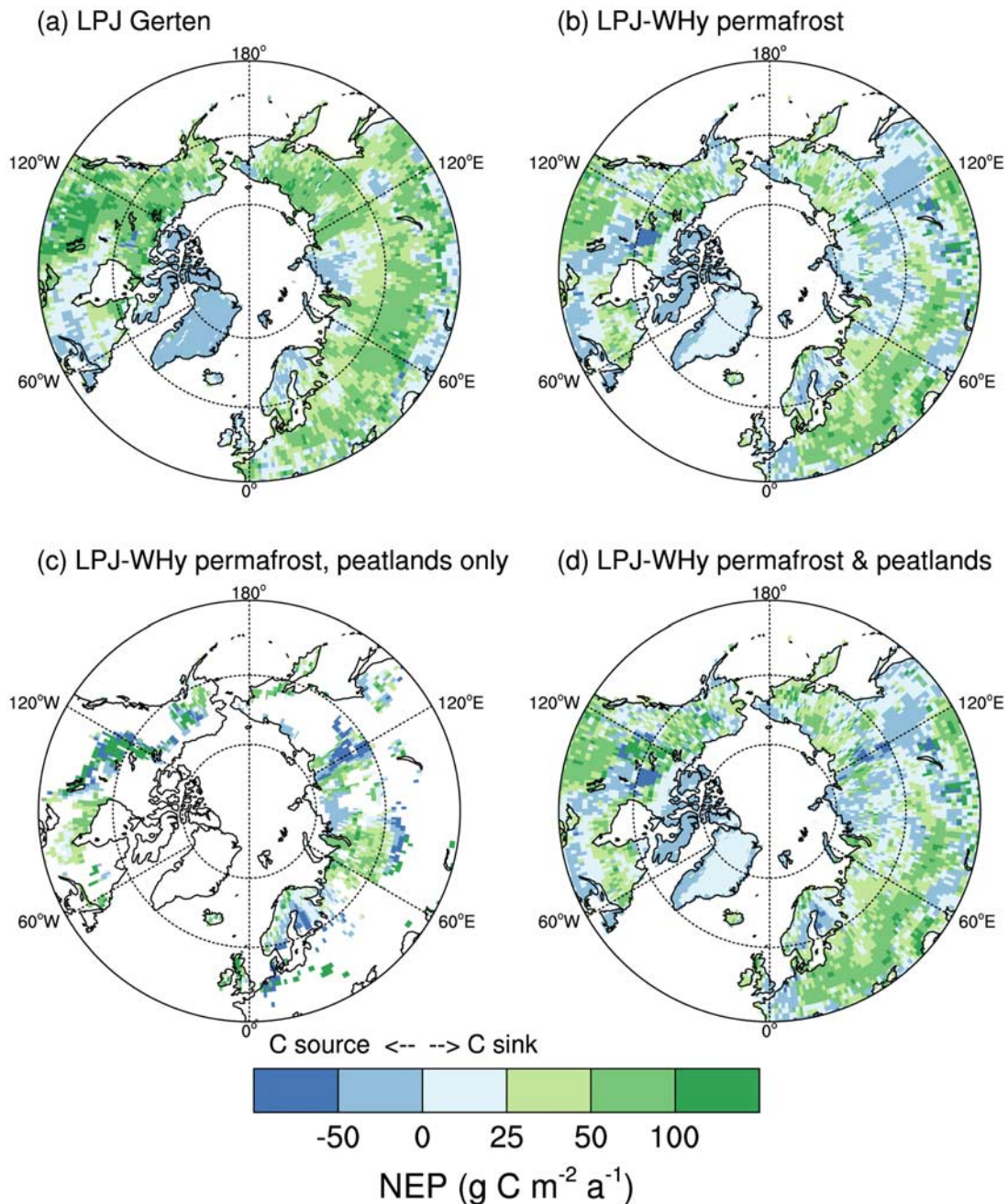


Figure 1. Annual simulated net ecosystem production (NEP) averaged over 1991–2000. (a) *Gerten et al.* [2004] version of LPJ, (b) all grid cells without peatland hydrology switched on, (c) peatland grid cells only, unweighted, and (d) overall NEP, combining generic and peatland values by weighting by fractional cover of peatlands. Regional summed values of NEP, where $\text{NEP} = \text{NPP} - \text{HR}$, for Figures 1a, 1b, and 1d are listed in Table 2.

[28] Figure 1c shows NEP for grid cells with organic soil. The highest peatland NEP was modeled in eastern Europe, the southern fringe of the West Siberian Lowlands, central Canada, and eastern Alaska. However, not all peatlands showed positive NEP values. Figure 1d shows the combined effect of including permafrost and peatlands. To produce this map, the model was run twice, once with and once without peatland hydrology. Overall results were calculated as a weighted average of the peatland and non-

peatland values, weighted by the fractional peatland cover for each grid cell (see part 1 [Wania et al., 2009, Figure S2]). The overall effect of adding peatlands to the permafrost is an increase in NEP compared to permafrost alone (Figure 1b versus Figure 1d) and a decrease in NEP compared to peatlands alone (Figure 1c versus Figure 1d).

[29] Figure 2 shows the frequency distribution of modeled and observed annual NEP for peatlands (observations as listed in Table 1). The simulated values peak at an NEP of

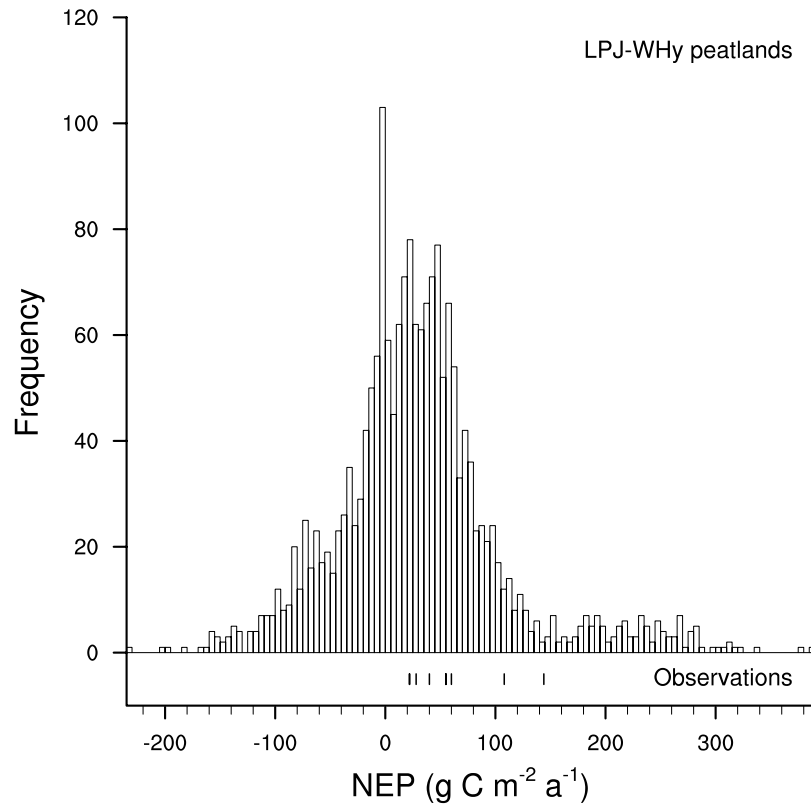


Figure 2. Histogram of annual NEP for peatland grid cells. References for observations (values shown as ticks below main histogram plot) are listed in Table 1.

-5 – 0 $\text{g C m}^{-2} \text{a}^{-1}$, but then extend towards higher values of 20 – 50 $\text{g C m}^{-2} \text{a}^{-1}$. The observations (based on CO_2 flux measurements) have a median of 40 $\text{g C m}^{-2} \text{a}^{-1}$. This comparison suggests that LPJ-WHy is capable of representing reasonable annual NEP values for peatlands.

4.3.2. Interannual Variability and Trends

[30] Figure 3 illustrates the sensitivity of modeled carbon fluxes to climate variability. The mean annual NPP of all grid cells for the 45 – 90°N region over the 1901–2002 time period is 14.9 Pg C , with a range from 13.6 to 17.0 Pg C . A clear positive trend over the century is visible

$$\text{NPP} = -29.470135 + 0.022736y, R^2 = 0.71, \quad (8)$$

where NPP is given in Pg C a^{-1} and y is the calendar year. This trend is significant at the 99% level: significance levels are 99% or greater throughout the paper, unless otherwise stated. The positive trend is at least partially caused by the rise in atmospheric CO_2 concentration over the course of the simulation. However, NPP is correlated not only with atmospheric CO_2 concentration, but also with soil temperature (correlation not shown). We conducted an experiment in which atmospheric CO_2 concentrations were held constant at 321 ppmv, i.e., the mean over 1901–2002. This resulted in a weaker NPP trend:

$$\text{NPP} = -1.140716 + 0.008309y, R^2 = 0.28, \quad (9)$$

with NPP again in Pg C a^{-1} . These results indicate that temperature plays only a minor role in the modeled NPP trend.

[31] Between 1901 and 2002, NEP fluctuated between around 0 and 1.7 Pg C a^{-1} , with a mean of 0.88 Pg C a^{-1} . Values for the global biosphere are estimated to be approximately 0.3 ± 0.9 Pg C a^{-1} for the 1980s [Prentice *et al.*, 2001] and 1.0 ± 0.6 Pg C a^{-1} for the 1990s [Prentice *et al.*, 2001; Denman *et al.*, 2007]. Sitch *et al.* [2008] reported results from five DGVMs, finding a mean global NEP minus fire carbon flux over the 1990s of 1.5 – 2.8 Pg C a^{-1} . LPJ-WHy's circumpolar mean NEP for the 1980s is 1.04 Pg C a^{-1} , of which 0.8 Pg C a^{-1} is lost because of fire. Peatlands contribute 0.14 Pg C a^{-1} to the circumpolar NEP, but fire consumes 0.058 Pg C a^{-1} , and the balance of accumulation and fire is 0.082 Pg C a^{-1} . Clymo *et al.* [1998] estimated the current carbon sequestration (i.e., NEP minus fire flux) by northern peatlands to be 0.067 Pg C a^{-1} .

[32] In contrast to NPP, NEP does not show a significant trend (Figure 3). As NPP rises, heterotrophic respiration also rises, although with a time lag, keeping NEP more or less stable. Heterotrophic respiration is correlated to CO_2 concentration, soil temperature, and NPP, whereas NEP is not correlated to any of these factors (not shown). However, when keeping atmospheric CO_2 constant over the course of the simulation, we observe a decline in NEP from about 1970 onwards (Figure S4), brought about by a stronger increase in HR compared to NPP. If these findings are realistic, they could have profound implications for the

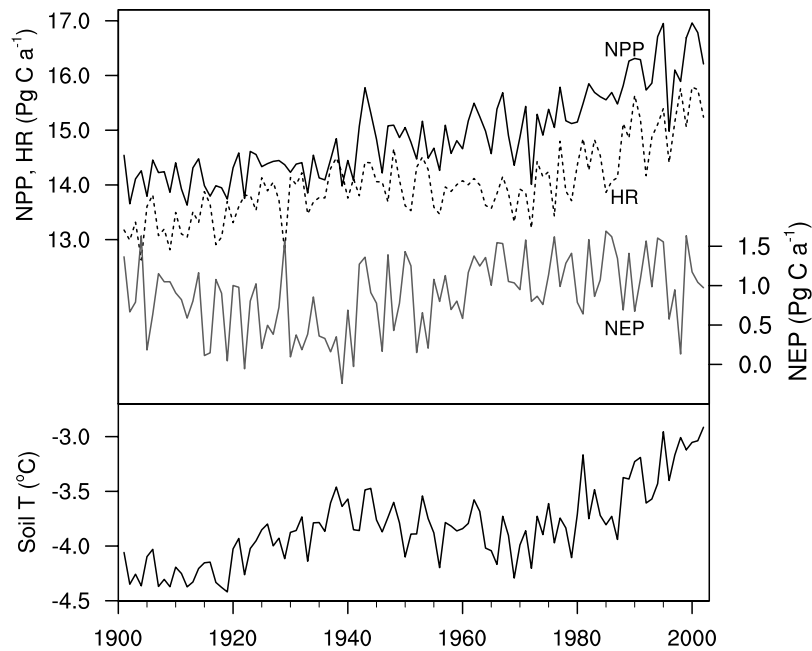


Figure 3. Interannual variability of net primary production (NPP), heterotrophic respiration (HR) and net ecosystem production (NEP) from 45–90°N, and soil temperature at 25 cm depth for the time period 1901–2002.

carbon balance in northern regions. In the future, photosynthesis will reach a saturation point at which additional CO_2 will not further enhance NPP, but as temperatures continue to rise, HR will also rise. When HR reaches a point where it starts to exceed NPP, NEP will become negative. Although this study does not consider the full NECB [Chapin *et al.*, 2006], it is clear that once NEP becomes negative, the total carbon balance will certainly be negative.

4.3.3. Seasonality

[33] Observed and modeled monthly NEP from four peatland sites are compared in Figure 4 (see Table 3 for the relevant statistics). There is a general overestimation of the amplitude of seasonal NEP variation in the model. The NEP observations range from -20 to $50 \text{ g C m}^{-2} \text{ month}^{-1}$, whereas the modeled NEP ranges from -90 to $120 \text{ g C m}^{-2} \text{ month}^{-1}$. The overestimation of the NEP range would be expected if NPP is overestimated. On the one hand, higher NPP values would contribute to greater positive NEP values in summer by sequestering more CO_2 . On the other hand, higher NPP would also lead to greater negative NEP in winter as more carbon is available for heterotrophic respiration. However, NEP is underestimated in August and September 1998 and 2001 and September 2002, when the modeled water table position was at its lower boundary of -300 mm for the Mer Bleue site. The simulated water table positions show a difference of 400 mm between their maximum value in spring and their lowest position in autumn, and this change is comparable to the observed drop of water table position [Lafleur *et al.*, 2005]. LPJ-WHy may thus exaggerate the drop in NPP because of a lower water table in a dry summer. The same pattern can be found at the Degerö site for September 2002, when the water table dropped leading to a reduction in NPP, while HR stayed

high, causing modeled NEP to plummet. Even though studies have examined the effects of flooding on the physiology of peatland plants [Pezeshki, 2001; Baird and Wilby, 1999, and references therein], few have looked at the effect of intermittent drought on peatland plants [Li *et al.*, 2004]. *Sphagnum* mosses are likely to experience drought stress relatively quickly [Clymo and Hayward, 1982], but

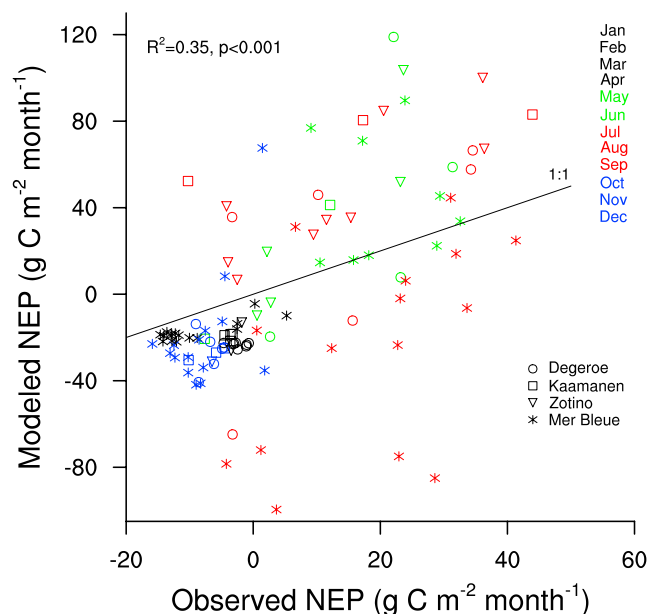


Figure 4. Observed versus modeled monthly NEP for four sites: Degerö, Sweden (2001–2002), Kaamanen, Finland (average over 1997–2002), Zotino, Russia (1998–2000), and Mer Bleue, Canada (1998–2002).

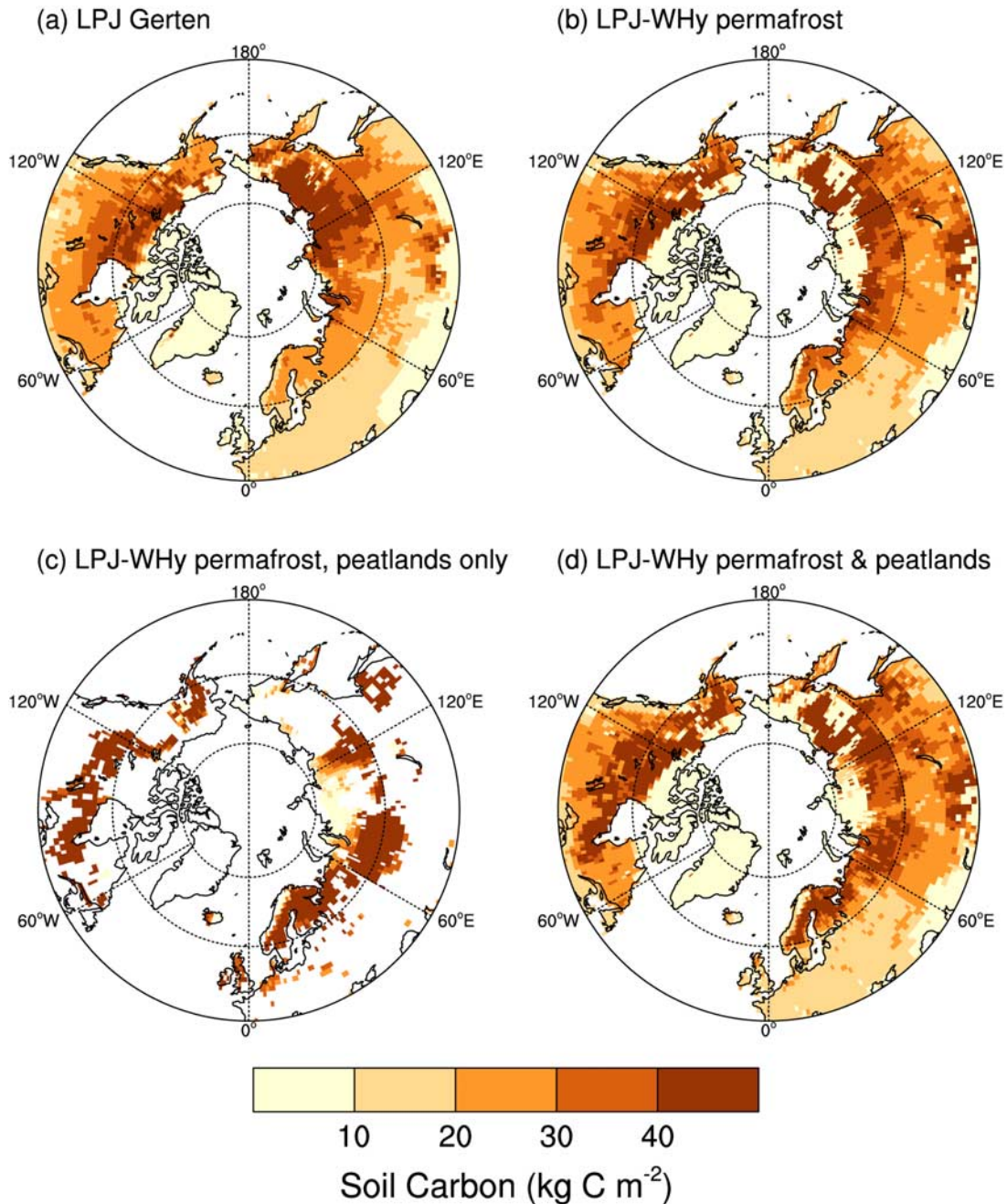


Figure 5. Annual simulated soil carbon averaged over 1991–2000. (a) *Gerten et al.* [2004] version of LPJ (891 Pg C), (b) all grid cells without peatland hydrology switched on (930 Pg C), (c) peatland grid cells only, unweighted (427 Pg C), and (d) overall soil carbon, combining generic and peatland values by weighting by fractional cover of peatlands (968 Pg C). Values in parentheses are the total carbon stored in soils from 45–90°N.

graminoids have roots that enable them to access water from deeper soil layers [Bernard and Fiala, 1986; Kohzu *et al.*, 2003] and may therefore cope better with lower water tables. More experimental work is needed to relate photosynthesis rates to fluctuations in water table position.

4.4. Soil Carbon

[34] Figure 5 shows differences in soil carbon content between the same four model configurations as used in

Figure 1. In North America, inclusion of permafrost causes a slight southward shift of high-carbon soils in arctic Canada and of soils with medium carbon content in southern central Canada. In Eurasia, the changes are larger, with higher carbon content in northern Scandinavia and the West Siberian Lowlands. The areas of Russia with low soil carbon become more extensive because of the effect of soil freezing on water availability [Beer *et al.*, 2007]. However, with the model peatland hydrology enabled, we find high

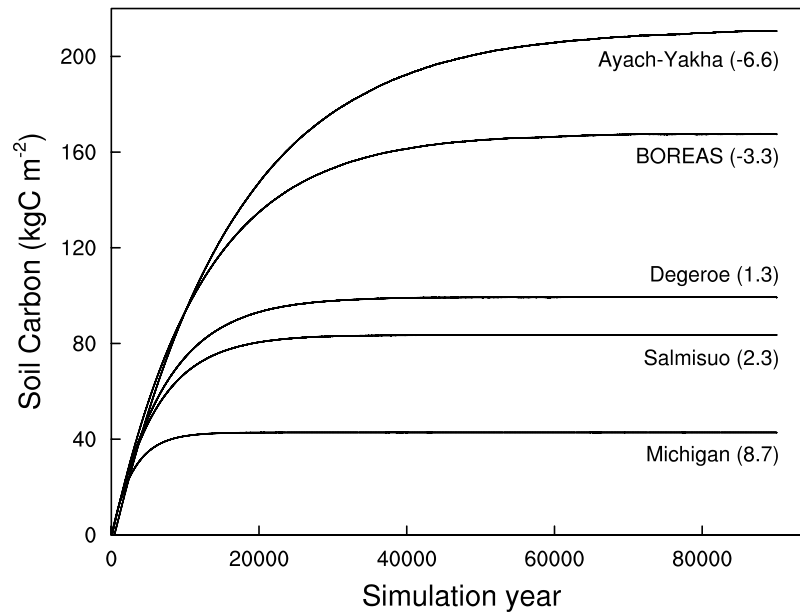


Figure 6. Soil carbon content for five sites through 90,102 years of simulation. Values in parentheses are mean annual air temperature in °C.

soil carbon contents in most peatlands (Figures 5c and 5d) because of the deceleration of decomposition. The modeled soil carbon content of 40–50 kg C m⁻² is lower than estimates of 96–133 kg C m⁻² reported in the literature [Gorham, 1991; Turunen *et al.*, 2002]. The explanation for the lower soil carbon contents lies in the relatively short spin-up time of LPJ-WHY.

[35] Soil carbon in nonpeatland grid cells reaches equilibrium after a few hundred years, so that a spin-up time of 1000 years is appropriate. However, peatlands accumulate carbon over long timescales and reach equilibrium only when carbon gained equals carbon lost [Clymo, 1984b]. The critical factor in this balance is the catotelm. As carbon accumulates in peatlands, the catotelm deepens. Decomposition in the catotelm is slow, but does occur, and once the catotelm is thick enough, it contributes enough respiration to counterbalance soil carbon gains. LPJ-WHY was run for a spin-up time of 90,000 years, plus 102 years of transient run, for five sites differing in mean annual temperature. Figure 6 shows the evolution of soil carbon over 90,102 years at these sites. Michigan, the warmest site, reaches 95% of its equilibrium value (40 kg C m⁻²) after less than 10,000 years. Ayach-Yakha, the coldest site, takes almost 50,000 years to reach 95% of its equilibrium value of >200 kg C m⁻². The correlation between mean annual air temperature, T_a (°C), and the final soil carbon content, C_{soil} (kg C m⁻²), is

$$C_{\text{soil}} = 126.385 - 11.26 T_a, R^2 = 0.96. \quad (10)$$

[36] The correlation between mean annual air temperature and time until 95% of the equilibrium soil carbon content is reached τ_{95} (years) is

$$\tau_{95} = 27774.8 - 2611.2 T_a, R^2 = 0.95. \quad (11)$$

[37] These correlations indicate a very close relationship between air temperature and soil carbon accumulation rate, in agreement with Clymo *et al.* [1998], who analyzed data from almost 800 sites in Finland and found a clear decrease in accumulation rates from south to north.

[38] Carbon accumulation in LPJ-WHY is influenced by the rate of flux of carbon from the acrotelm to the catotelm (see section 2.5), currently set to 12 g C m⁻² a⁻¹ [Clymo, 1984b]. In addition, a small fraction of freshly accumulated litter (1.5%) is added to the slow carbon pool. A commonly used term in the peatland research community is the “long-term apparent rate of carbon accumulation” (LORCA). Reported values of LORCA (in g C m⁻² a⁻¹) are 14.0 ± 3.7 to 21.9 ± 2.8 for the interval from 400 to 3000 years ago for two cores at Mer Bleue, Canada [Roulet *et al.*, 2007], and 18.5 for undrained Finnish mires [Turunen *et al.*, 2002], where the lowest values were found in fens (16.9), and the highest values were found in raised bogs (26.1). The LORCA values for Mer Bleue compared well to a 6-year-long mass balance study resulting in a carbon sink of 21.5 ± 39.0 g C m⁻² a⁻¹ [Roulet *et al.*, 2007]. However, Tolonen and Turunen [1996] found that the true rate of carbon accumulation is only about 60% of LORCA, which would bring the rate of carbon accumulation down to 8.4–13.1 g C m⁻² a⁻¹, similar to the value of 12 g C m⁻² a⁻¹ used in this work.

[39] In summary, LPJ-WHY can accumulate peat realistically in the form of carbon storage in the slow carbon pool. The accumulation continues until a stable state is reached, at which point the contribution of heterotrophic respiration is large enough that the NEP is close to zero. The time taken for a system to approach this steady state depends on the mean annual air temperature. None of the five sites tested above were in soil carbon equilibrium after the standard spin-up time of 1000 years. One key unknown prevents us from modeling total column carbon content more realisti-

cally, namely the time since peat initialization. What we need is a complete gridded data set of peat initialization similar to that shown by *MacDonald et al.* [2006]. Further work in this direction is underway, and spatial data may be available to the modeling community soon (P. Oksanen, personal communication, 2008).

[40] The estimate of carbon stored in peatland soil is 270–500 Pg C [*Gorham*, 1991; *Maltby and Immerzi*, 1993; *Davidson and Janssens*, 2006; *Turunen et al.*, 2002], while LPJ-WHy simulates 427 Pg C. However, the peatland map used for our study overestimates peatland area by a factor of 1.67 relative to *Aselman and Crutzen* [1989] and 2.61 relative to the map of *Prigent et al.* [2007]. If we correct the peatland area downwards, we obtain a corresponding circumpolar peatland soil carbon content of 164–256 Pg C. These values are at the lower limit of current estimates, but are derived from simulations where spin-up time was limited to 1000 years. We expect soil carbon content to rise as the spin-up time lengthens until we reach equilibrium conditions at all points. We thus expect our estimate of total carbon in peatlands to be somewhat low.

4.5. Effect of Spin-up Duration on NEP

[41] The length of the spin-up procedure influences NEP by increasing heterotrophic respiration from the growing slow carbon pool. The length of the spin-up period matters only until the soil carbon has reached equilibrium. For nonpeatland sites, an equilibrium is established after 1000 years by the use of an analytical solution for the exponential carbon accumulation. In order to test the potential bias of peatland NEP when limiting spin-up to 1000 years, the same spin-up comparison simulations used to produce Figure 6 were used to calculate NPP, HR, and NEP values for comparison between the 1000 year and 90,000 year spin-up approaches (Table S3). NEP did not differ significantly between the 1 k and 90 k runs at the three warmer sites (Michigan, Salmisuo, and Degerö), but showed greater differences at the two colder sites (BOREAS and Ayach-Yakha). For the two latter sites, a significant difference was found in HR but not in NPP. This is as expected since HR depends on carbon pool size while NPP does not.

[42] For sites in colder areas, it will therefore be important to consider the site's history when assessing simulated NEP. The BOREAS site has positive NEP after the 1k spin-up, but is close to zero after the 90 k spin-up. The Ayach-Yakha site is more extreme, switching from a strong positive NEP to a negative NEP from the 1 k to the 90 k spin-up.

4.6. Sensitivity Experiment

[43] In order to test the sensitivity of vegetation dynamics to changes in climate, six sites were chosen, and LPJ-WHy simulations were performed for different climate conditions, independently increasing the monthly mean air temperature and monthly precipitation across ranges selected to correspond to changes projected by an ECHAM5 GCM simulation forced by the IPCC SRES A2 emissions scenario. The results of experiments using an atmospheric CO₂ concentration of 780 ppmv are shown in Figure 7, and for comparison, results of experiments using CO₂ concentration

of 380 ppmv are shown in Figure S5. The results may be examined in conjunction with the land surface process sensitivity experiments in part 1 [*Wania et al.*, 2009].

[44] Figure 7a shows projected changes of mean annual air temperature by the end of this century under the SRES A2 scenario. This was used to guide the setup of the sensitivity experiment. The six sites chosen are located in areas that experience temperature increases of 4 to >7°C. Figure 7b shows the change in NPP under precipitation (ΔP) and temperature increases (ΔT). The starting NPP values (bottom left corner of each individual panel) are under 300 g C m⁻² a⁻¹ for sites 1, 4, and 6, 300–400 g C m⁻² a⁻¹ for sites 3 and 5, and over 600 g C m⁻² a⁻¹ for site 2. These results are obtained using an atmospheric CO₂ concentration of 780 ppmv and are therefore somewhat higher than present-day values. When using an atmospheric CO₂ concentration of only 380 ppmv, the starting NPP for site 2 is between 500 and 600 g C m⁻² a⁻¹ (Figure S5). Higher NPP values at 780 ppmv are mainly caused by an increase in vascular plant NPP, whereas *Sphagnum* mosses either show a slight increase or a decrease due to complex interactions between *Sphagnum* moss growth and water table position or due to competition with other PFTs.

[45] Sites 1, 3, 4, and 5 show an increase in NPP as temperature rises, but increases in precipitation have only a minor impact. In contrast, site 2 shows a decline in NPP followed by an increase as temperatures are increased under conditions of constant precipitation. However, when temperature and precipitation increase together, the precipitation changes outweigh the effects of rising temperatures and NPP remains constant (dashed lines in Figure 7, which connect starting conditions with end conditions as projected for 2100 by ECHAM5). This pattern observed for site 2 reflects the changes in water table position shown in part 1 [*Wania et al.*, 2009]. The increase of NPP above 6°C at 0% ΔP and at 9°C with 10% ΔP is due to a change in vegetation. While ΔT is low or ΔP is high, water tables remain high and support peatland PFTs. However, when ΔT reaches 6°C without any increase in precipitation, water tables drop far enough to allow tree or C₃ grass PFTs to survive. This transition in vegetation is also seen at site 6, where a diagonal zone of lower net productivity separates two zones of higher NPP, which again tallies nicely with the pattern of water table positions in part 1 [*Wania et al.*, 2009].

[46] Heterotrophic respiration, shown in Figure 7c, behaves similarly to NPP. Variations in water table position do not influence these results, as the moisture response in peatlands in LPJ-WHy is fixed (equation (6)).

[47] The variable of most interest is NEP, shown in Figure 7d. Sites 3 and 4 increase from a “neutral” NEP to a clearly positive NEP along the trajectory of future climate conditions, as indicated by the dashed lines in each panel. Site 5 appears to be stable over almost the entire temperature and precipitation range examined, with a decrease in NEP under only the warmest and driest conditions. Site 1 shows a strong increase in NEP with temperature from 100–150 g C m⁻² a⁻¹ to over 200 g C m⁻² a⁻¹. NEP decreases with increasing precipitation, but at the greatest ΔP , values increases again. This

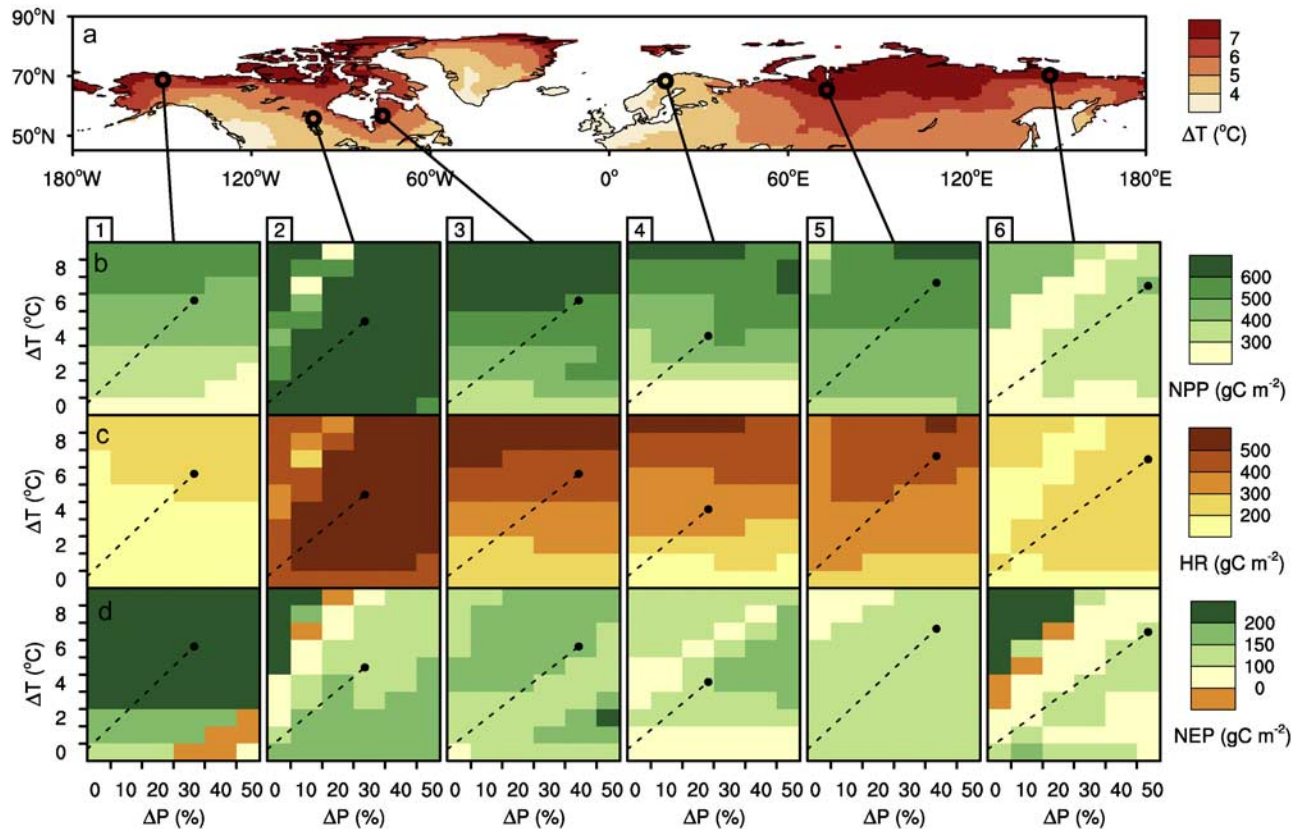


Figure 7. Sensitivity of net primary production (NPP), heterotrophic respiration (HR), and net ecosystem production (NEP) at six sites (Table 6 in part 1 [Wania *et al.*, 2009]) in different zones of projected temperature increase under an atmospheric CO_2 mixing ratio of 780 ppmv. (a) Temperature change projected by the ECHAM5 GCM under the IPCC SRES A2 emissions scenario: this was derived by averaging the 30-year mean for 2071–2100 over the three ECHAM5 ensemble runs and subtracting the 30-year mean over the three ensembles for 1961–1990. (b–d) Absolute values of (Figure 7b) net primary production, (Figure 7c) heterotrophic respiration, and (Figure 7d) net ecosystem production as air temperature and precipitation change. The dots on Figures 7b–7d indicate climate conditions at each site for the year 2100 projected by ECHAM5 GCM simulations driven by the IPCC SRES A2 scenario. The dashed line shows a possible trajectory from present-day to projected 2100 conditions, assuming that temperature and precipitation change in concert.

pattern can be explained by a rising water table which enables the growth of peatland PFTs (not shown), leading to lower NEP because the NPP of peatland PFTs is lower than that of generic PFTs (indirectly seen in Figure 7b by the decrease in NPP at ΔT of 0–2 $^{\circ}\text{C}$ and ΔP of 30–50%). Sites 2 and 6 also experience a change in vegetation composition due to a large drop in water table (see Figure 7 in part 1 [Wania *et al.*, 2009]). Under cooler and wetter conditions, when water tables are high, peatland PFTs thrive, while under warmer and drier conditions, when water tables are low, generic PFTs grow. Interestingly, NEP is higher when generic PFTs are present (top left corner of sites 2 and 6 in Figure 7d). This effect is caused by slightly higher NPP combined with lower HR. The model's behavior in simulating lower respiration under lower water table conditions is plausible, as lower water tables coincide with lower soil temperatures (not shown), reducing the rate of respiration. Finally, we would like to add a word of caution concerning the interpretation of the sensitivity

results. Model PFTs experience increases in CO_2 , temperature, and precipitation, without any limitation in mineral nutrients. In the real world, plant growth is limited primarily by nitrogen and phosphorous availability, and it is questionable whether nutrient supply under changing environmental conditions will keep up with plant demand.

5. Conclusions

[48] The introduction of permafrost into LPJ-WHY had a strong impact on the simulation of NEP and soil carbon storage in some of the coldest areas of the circumpolar region, where the lack of freezing water permitted too much productivity in previous model versions. The addition of peatlands further reduced NPP, but had only a small positive effect on circumpolar NEP. Both permafrost and peatlands increased the soil carbon content of the circumpolar region, a crucial element for future projections of the global terrestrial carbon cycle. There is much uncertainty

concerning the future of the terrestrial carbon sink [Friedlingstein et al., 2006]. Inclusion of permafrost and peatlands into models will have implications for the simulation of this carbon sink.

[49] LPJ-WHY is able to simulate the seasonality of NEP realistically, but not its amplitude. We speculate that this is due to overestimation of NPP, possibly due to lack of nutrient limitation in the model. Photosynthesis is generally lower in plants growing in peatlands compared to similar plants growing in other ecosystems [Arneeth et al., 2006]. This is presumably caused by lack of nutrients, most likely nitrogen, lack of oxygen, accumulation of phytotoxins, or by a combination of these factors [Pezeshki, 2001; Cronk and Fennessy, 2001]. Long-term trends in NPP and heterotrophic respiration are visible over the last third of the 20th century. The increase in NPP is mainly driven by increasing atmospheric CO₂ concentrations, while the increase of heterotrophic respiration is caused by rising temperatures.

[50] Modeled annual NEP of peatlands was shown to lie within the range of observations. This means that our simple future sensitivity experiment has some validity, despite deficiencies in the current model. The general trend projected by our experiment is towards higher NPP and heterotrophic respiration and slightly higher NEP in a warmer, high-CO₂ climate. The addition of methane emissions from peatlands is the next step in LPJ-WHY development [Wania, 2007] and will provide further insight into the changing carbon and greenhouse gas balance of boreal peatlands.

[51] **Acknowledgments.** We thank Nigel Roulet, Peter Lafleur, and Elyn Humphreys of the NSERC-CFCAS/Fluxnet Canada (Canadian Carbon Project Mer Bleue observatory) for the provision of NEE data for the Mer Bleue site. We thank Mats Nilson and Jörgen Sagerfors for providing NEE data for the Degerö site, funded by Swedish Research Council for Environment (grant 621-2001-1911), Agricultural Sciences and Spatial Planning (grant 21.4/2003-0876), and the Kempe Foundation for grants for the micrometeorological instruments. We acknowledge the modeling groups, the Program for Climate Model Diagnosis and Intercomparison (PCMDI), and the WCRP's Working Group on Coupled Modelling (WGCM) for their roles in making available the WCRP CMIP3 multimodel data set. Support of this data set is provided by the Office of Science, U.S. Department of Energy. We acknowledge the valuable input by Paul Miller on code development and manuscript preparation. We thank Renato Spahni for help with the provision of the IGBP-DIS soil carbon data, Angela Gallego-Sala for discussion of the manuscript, Paul Valdes for the provision of computer facilities time, and Gethin Williams for IT support. R.W. was sponsored by a studentship of the Department of Earth Sciences, University of Bristol, and by the EU-Project HYMN (GOCE-037048). I.R. was supported by a NERC e-Science studentship (NER/S/G/2005/13913). The manuscript has greatly improved after reviews by Nigel Roulet and an anonymous reviewer.

References

- Aerts, R., J. T. A. Verhoeven, and D. F. Whigham (1999), Plant-mediated controls on nutrient cycling in temperate fens and bogs, *Ecology*, *80*(7), 2170–2181.
- Arneeth, A., E. M. Veenendaal, C. Best, W. Timmermans, O. Kolle, L. Montagnani, and O. Shibistova (2006), Water use strategies and ecosystem-atmosphere exchange of CO₂ in two highly seasonal environments, *Biogeosciences*, *3*(4), 421–437.
- Aselman, I., and P. J. Crutzen (1989), Global distribution of natural freshwater wetlands and rice paddies, and their net primary productivity, seasonality and possible methane emissions, *J. Atmos. Chem.*, *8*, 307–358.
- Aurela, M., T. Laurila, and J. P. Tuovinen (2004), The timing of snow melt controls the annual CO₂ balance in a subarctic fen, *Geophys. Res. Lett.*, *31*, L16119, doi:10.1029/2004GL020315.
- Baird, A. J., and R. L. Wilby (Eds.) (1999), *Eco-Hydrology: Plants and Water in Terrestrial and Aquatic Environments*, Routledge Phys. Environ. Ser., Routledge, London.
- Beer, C., W. Lucht, D. Gerten, K. Thonicke, and C. Schmullius (2007), Effects of soil freezing and thawing on vegetation carbon density in Siberia: A modeling analysis with the Lund-Potsdam-Jena Dynamic Global Vegetation Model, *Global Biogeochem. Cycles*, *21*, GB1012, doi:10.1029/2006GB002760.
- Bernard, J. M., and K. Fiala (1986), Distribution and standing crop of living and dead roots in three wetland *Carex* species, *Bull. Torrey Bot. Club*, *113*(1), 1–5.
- Bragazza, L., R. Gerdol, and H. Rydin (2003), Effects of mineral and nutrient input on mire bio-geochemistry in two geographical regions, *J. Ecol.*, *91*(3), 417–426.
- Bragazza, L., et al. (2005), Nitrogen concentration and δ¹⁵N signature of ombrotrophic Sphagnum mosses at different N deposition levels in Europe, *Global Change Biol.*, *11*(1), 106–114.
- Bridgham, S. D., J. P. Megonigal, J. K. Keller, N. B. Bliss, and C. Trettin (2006), The carbon balance of North American wetlands, *Wetlands*, *26*(4), 889–916.
- Chanton, J. P., J. E. Bauer, P. A. Glaser, D. I. Siegel, C. A. Kelley, S. C. Tyler, E. H. Romanowicz, and A. Lazrus (1995), Radiocarbon evidence for the substrates supporting methane formation within northern Minnesota peatlands, *Geochim. Cosmochim. Acta*, *59*(17), 3663–3668.
- Chapin, F. S., et al. (2006), Reconciling carbon-cycle concepts, terminology, and methods, *Ecosystems*, *9*(7), 1041–1050.
- Christensen, J. H., et al. (2007), Regional climate projections, in *Climate Change 2007: The Physical Science Basis. Contribution of Working Group I to the Fourth Assessment Report of the Intergovernmental Panel on Climate Change*, edited by S. Solomon et al., chap. 11, pp. 847–940, Cambridge Univ. Press, Cambridge, U. K.
- Christensen, T. R., A. Ekberg, L. Ström, M. Mastepanov, N. Panikov, M. Öquist, B. H. Svensson, H. Nykänen, P. J. Martikainen, and H. Oskarsson (2003), Factors controlling large scale variations in methane emissions from wetlands, *Geophys. Res. Lett.*, *30*(7), 1414, doi:10.1029/2002GL016848.
- Clymo, R. S. (1984a), *Sphagnum*-dominated peat bog: A naturally acid ecosystem, *Philos. Trans. R. Soc. Lond., B*, *305*(1124), 487–499.
- Clymo, R. S. (1984b), The limits to peat bog growth, *Philos. Trans. R. Soc. Lond., B*, *303*(1117), 605–654.
- Clymo, R. S., and P. M. Hayward (1982), The ecology of *Sphagnum*, in *Bryophyte Ecology*, edited by A. J. E. Smith, pp. 229–289, Chapman and Hall, London.
- Clymo, R. S., J. Turunen, and K. Tolonen (1998), Carbon accumulation in peatland, *Oikos*, *81*(2), 368–388.
- Colmer, T. D. (2003), Long-distance transport of gases in plants: A perspective on internal aeration and radial oxygen loss from roots, *Plant Cell Environ.*, *26*, 17–36.
- Cronk, J. K., and M. S. Fennessy (2001), *Wetland Plants: Biology and Ecology*, CRC Press LLC, Boca Raton, Fla.
- Davidson, E. A., and I. A. Janssens (2006), Temperature sensitivity of soil carbon decomposition and feedbacks to climate change, *Nature*, *440*, 165–173.
- Denman, K. L., et al. (2007), Couplings between changes in the climate system and biogeochemistry, in *Climate Change 2007: The Physical Science Basis. Contribution of Working Group I to the Fourth Assessment Report of the Intergovernmental Panel on Climate Change*, edited by S. Solomon et al., chap. 7, pp. 499–588, Cambridge Univ. Press, Cambridge, U. K.
- Etheridge, D. M., L. P. Steele, R. L. Langenfelds, R. J. Francey, J. M. Barnola, and V. I. Morgan (1996), Natural and anthropogenic changes in atmospheric CO₂ over the last 1000 years from air in antarctic ice and firn, *J. Geophys. Res.*, *101*(D2), 4115–4128.
- Evans, D. E. (2003), *Tansley review: Aerenchyma formation*, *New Phytol.*, *161*, 35–49.
- FAO (1991), The digitized soil map of the world (release 1.0), *Tech. Rep. 67/1*, Food and Agricul. Org. of the U. N..
- Freeman, C., N. Ostle, and H. Kang (2001), An enzymic “latch” on a global carbon store, *Nature*, *409*, 149.
- Frenzel, P., and J. Rudolph (1998), Methane emission from a wetland plant: The role of CH₄ oxidation in *Eriophorum*, *Plant Soil*, *202*(1), 27–32.
- Friborg, T., H. Soegaard, T. R. Christensen, C. R. Lloyd, and N. S. Panikov (2003), Siberian wetlands: Where a sink is a source, *Geophys. Res. Lett.*, *30*(21), 2129, doi:10.1029/2003GL017797.
- Friedlingstein, P., et al. (2006), Climate-carbon cycle feedback analysis: Results from the C⁴MIP model intercomparison, *J. Clim.*, *19*(14), 3337–3353.

- Gerten, D., S. Schaphoff, U. Haberlandt, W. Lucht, and S. Sitch (2004), Terrestrial vegetation and water balance: Hydrological evaluation of a dynamic global vegetation model, *J. Hydrol.*, 286, 249–270.
- Global Soil Data Task Group (2000), *Global Gridded Surfaces of Selected Soil Characteristics (IGBP-DIS)*, Oak Ridge Natl. Lab. Distrib. Active Archive Cent., Oak Ridge, Tenn. (Available at <http://www.daac.ornl.gov>)
- Gorham, E. (1991), Northern peatlands: Role in the carbon cycle and probable responses to climatic warming, *Ecol. Appl.*, 1(2), 182–195.
- Haxeltine, A., and I. C. Prentice (1996), BIOME3: An equilibrium terrestrial biosphere model based on ecophysiological constraints, resource availability, and competition among plant functional types, *Global Biogeochem. Cycles*, 10(4), 693–709.
- Helal, H. M., and D. R. Sauerbeck (1984), Influence of plant roots on C and P metabolism in soil, *Plant Soil*, 76(1–3), 175–182.
- Hütsch, B. W., J. Augustin, and W. Merbach (2002), Plant rhizodeposition: An important source for carbon turnover in soils, *J. Plant Nutr. Soil Sci.*, 165(4), 397–407.
- Ingram, H. A. P. (1983), Hydrology, in *Mires: Swamp, Bog, Fen and Moor*, edited by A. J. P. Gore, pp. 67–158, Elsevier, Amsterdam.
- Keeling, C. D., and T. P. Whorf (2005), Atmospheric CO₂ records from sites in the SIO air sampling network, in *Trends: A Compendium of Data on Global Change*, digital data, Carbon Dioxide Inf. Anal. Cent., Oak Ridge Natl. Lab., Oak Ridge, Tenn. (Available at <http://cdiac.esd.ornl.gov/trends/co2/sio-mlo.html>)
- Kohzu, A., K. Matsui, T. Yamada, A. Sugimoto, and N. Fujita (2003), Significance of rooting depth in mire plants: Evidence from natural ¹⁵N abundance, *Ecol. Res.*, 18(3), 257–266.
- Lafleur, P. M., T. J. Griffis, and W. R. Rouse (2001), Interannual variability in net ecosystem CO₂ exchange at the arctic treeline, *Arct. Antarct. Alp. Res.*, 33(2), 149–157.
- Lafleur, P. M., R. A. Hember, S. W. Admiral, and N. T. Roulet (2005), Annual and seasonal variability in evapotranspiration and water table at a shrub-covered bog in southern Ontario, Canada, *Hydrol. Process.*, 19(18), 3533–3550.
- Lamers, L. P. M., C. Farhoush, J. M. V. Groenendaal, and J. G. M. Roelofs (1999), Calcareous groundwater raises bogs: the concept of ombrotrophy revisited, *J. Ecol.*, 87(4), 639–648.
- Larcher, W. (2003), *Physiological Plant Ecology: Ecophysiology and Stress Physiology of Functional Groups*, 4th ed., Springer, New York.
- Li, S. W., S. R. Pezeshki, and S. Goodwin (2004), Effects of soil moisture regimes on photosynthesis and growth in cattail (*Typha latifolia*), *Acta Oecol.*, 25(1–2), 17–22.
- Lloyd, J., and J. A. Taylor (1994), On the temperature dependence of soil respiration, *Funct. Ecol.*, 8, 315–323.
- Lund, M., A. Lindroth, T. R. Christensen, and L. Ström (2007), Annual CO₂ balance of a temperate bog, *Tellus, Ser. B*, 59, 804–811.
- MacDonald, G. M., D. W. Beilman, K. V. Kremenetski, Y. Sheng, L. C. Smith, and A. A. Velichko (2006), Rapid early development of circumarctic peatlands and atmospheric CH₄ and CO₂ variations, *Science*, 314, 285–288.
- Malmer, N., and B. Wallen (2005), Nitrogen and phosphorus in mire plants: variation during 50 years in relation to supply rate and vegetation type, *Oikos*, 109, 539–554.
- Maltby, E., and P. Immirzi (1993), Carbon dynamics in peatlands and other wetland soils: Regional and global perspectives, *Chemosphere*, 27(6), 999–1023.
- Meehl, G. A., C. C. T. Delworth, M. Latif, B. McAvaney, J. F. B. Mitchell, R. J. Stouffer, and K. E. Taylor (2007a), The WCRP CMIP3 multi-model dataset: A new era in climate change research, *Bull. Am. Met. Soc.*, 88, 1383–1394.
- Meehl, G. A., et al. (2007b), Global climate projections, in *Climate Change 2007: The Physical Science Basis. Contribution of Working Group I to the Fourth Assessment Report of the Intergovernmental Panel on Climate Change*, edited by S. Solomon et al., chap. 10, pp. 747–846, Cambridge Univ. Press, Cambridge, U. K.
- Mitchell, T. D., and P. D. Jones (2005), An improved method of constructing a database of monthly climate observations and associated high-resolution grids, *Int. J. Climatol.*, 25(6), 693–712.
- Moore, T. R., J. L. Bubier, S. E. Frohling, P. M. Lafleur, and N. T. Roulet (2002), Plant biomass and production and CO₂ exchange in an ombrotrophic bog, *J. Ecol.*, 90(1), 25–36.
- New, M., M. Hulme, and P. D. Jones (1999), Representing twentieth century space-time climate variability. Part 1: Development of a 1961–1990 mean monthly terrestrial climatology, *J. Clim.*, 12, 829–856.
- Nungesser, M. K. (2003), Modelling microtopography in boreal peatlands: Hummocks and hollows, *Ecol. Model.*, 165(2–3), 175–207.
- Pezeshki, S. R. (2001), Wetland plant responses to soil flooding, *Environ. Exp. Bot.*, 46(3), 299–312.
- Prentice, I. C., G. D. Farquhar, M. J. R. Fasham, M. L. Goulden, M. Heimann, V. J. Jaramillo, H. S. Khashgi, C. Le Qur, R. J. Scholes, and D. W. R. Wallace (2001), The carbon cycle and atmospheric carbon dioxide, in *Climate Change 2001: The Scientific Basis. Contributions of Working Group I to the Third Assessment Report of the Intergovernmental Panel on Climate Change*, edited by L. F. Pitelka and A. R. Rojas, pp. 183–237, Cambridge Univ. Press, Cambridge, U. K.
- Prigent, C., F. Papa, F. Aires, W. B. Rossow, and E. Matthews (2007), Global inundation dynamics inferred from multiple satellite observations, 1993–2000, *J. Geophys. Res.*, 112, D12107, doi:10.1029/2006JD007847.
- R Development Core Team (2008), *R: A Language and Environment for Statistical Computing*, R Found. for Stat. Comput., Vienna, Austria.
- Robinson, S. D., and T. R. Moore (2000), The influence of permafrost and fire upon carbon accumulation in high boreal peatlands, Northwest Territories, Canada, *Arct. Antarct. Alp. Res.*, 32(2), 155–166.
- Roelofs, J. G. M., J. A. A. R. Schuurkes, and A. J. M. Smits (1984), Impact of acidification and eutrophication on macrophyte communities in soft waters: II. Experimental studies, *Aquat. Bot.*, 18, 389–411.
- Roulet, N. T., P. M. Lafleur, P. J. H. Richard, T. R. Moore, E. R. Humphreys, and J. Bubier (2007), Contemporary carbon balance and late Holocene carbon accumulation in a northern peatland, *Global Change Biol.*, 13(2), 397–411.
- Sagerfors, J., A. Lindroth, A. Grelle, L. Klemendsson, P. Weslien, and M. Nilsson (2008), Annual CO₂ exchange between a nutrient-poor, minerotrophic boreal mire and the atmosphere, *J. Geophys. Res.*, 113, G01001, doi:10.1029/2006JG000306.
- Segers, R. (1998), Methane production and methane consumption: a review of processes underlying wetland methane fluxes, *Biogeochemistry*, 41(1), 23–51.
- Silvola, J. (1991), Moisture dependence of CO₂ exchange and its recovery after drying in certain boreal forest and peat mosses, *Lindbergia*, 17, 5–10.
- Silvola, J., and H. Aaltonen (1984), Water content and photosynthesis in the peat mosses *Sphagnum fuscum* and *Sphagnum angustifolium*, *Ann. Bot. Fenn.*, 21(1), 1–6.
- Sitch, S., et al. (2003), Evaluation of ecosystem dynamics, plant geography and terrestrial carbon cycling in the LPJ dynamic global vegetation model, *Global Change Biol.*, 9(2), 161–185.
- Sitch, S., et al. (2008), Evaluation of the terrestrial carbon cycle, future plant geography and climate-carbon cycle feedbacks using five Dynamic Global Vegetation Models (DGVMS), *Global Change Biol.*, 14, 2015–2039, doi:10.1111/j.1365-2486.2008.01626.x.
- Smith, B., I. C. Prentice, and M. T. Sykes (2001), Representation of vegetation dynamics in the modelling of terrestrial ecosystems: Comparing two contrasting approaches within European climate space, *Global Ecol. Biogeogr.*, 10(6), 621–637.
- Smolders, A. J. P., H. B. M. Tomassen, H. W. Pijnappel, L. P. M. Lamers, and J. G. M. Roelofs (2001), Substrate-derived CO₂ is important in the development of *Sphagnum* spp., *New Phytol.*, 152(2), 325–332.
- Sottocornola, M., and G. Kiely (2005), An Atlantic blanket bog is a modest CO₂ sink, *Geophys. Res. Lett.*, 32, L23804, doi:10.1029/2005GL024731.
- St-Hilaire, F., J. Wu, N. T. Roulet, S. Frohling, P. M. Lafleur, E. R. Humphreys, and V. Arora (2008), McGill wetland model: Evaluation of a peatland carbon simulator developed for global assessments, *Biogeosci. Disc.*, 5, 1689–1725.
- Stöckli, R., D. M. Lawrence, G.-Y. Niu, K. W. Oleson, P. E. Thornton, Z.-L. Yang, G. B. Bonan, A. S. Denning, and S. W. Running (2008), Use of FLUXNET in the Community Land Model development, *J. Geophys. Res.*, 113, G01025, doi:10.1029/2007JG000562.
- Ström, L., M. Mastepanov, and T. R. Christensen (2005), Species-specific effects of vascular plants on carbon turnover and methane emissions from wetlands, *Biogeochemistry*, 75, 65–82.
- Syed, K. H., L. B. Flanagan, P. J. Carlson, A. J. Glenn, and K. E. V. Gaalen (2006), Environmental control of net ecosystem CO₂ exchange in a treed, moderately rich fen in northern Alberta, *Agr. For. Meteorol.*, 140(1–4), 97–114.
- Thonicke, K., S. Venevsky, S. Sitch, and W. Cramer (2001), The role of fire disturbance for global vegetation dynamics: Coupling fire into a Dynamic Global Vegetation Model, *Global Ecol. Biogeogr.*, 10(6), 661–677.
- Thormann, M. N., S. E. Bayley, and A. R. Szumigalski (1998), Effects of hydrologic changes on aboveground production and surface water chemistry in two boreal peatlands in Alberta: Implications for global warming, *Hydrobiologia*, 362, 171–183.
- Titus, J. E., D. J. Wagner, and M. D. Stephens (1983), Contrasting water relations of photosynthesis for 2 *Sphagnum* mosses, *Ecology*, 64(5), 1109–1115.

- Tolonen, K., and J. Turunen (1996), Accumulation rates of carbon in mires in Finland and implications for climate change, *Holocene*, 6(2), 171–178.
- Turunen, J., E. Tomppo, K. Tolonen, and A. Reinikainen (2002), Estimating carbon accumulation rates of undrained mires in Finland: Application to boreal and subarctic regions, *Holocene*, 12(1), 69–80.
- Wania, R. (2007), Modelling northern peatland land surface processes, vegetation dynamics and methane emissions, Ph.D. thesis, Univ. of Bristol, Bristol, U. K.
- Wania, R., I. Ross, and I. C. Prentice (2009), Integrating peatlands and permafrost into a dynamic global vegetation model: 1. Evaluation and sensitivity of physical land surface processes, *Global Biogeochem. Cycles*, 23, GB3014, doi:10.1029/2008GB003412.
- Wheeler, B. D. (1999), Water and plants in freshwater wetlands, in *Eco-Hydrology: Plants and Water in Terrestrial and Aquatic Environments*, edited by A. J. Baird and R. L. Wilby, pp. 127–180, Routledge Phys. Environ. Ser., Routledge, London.
- Whipps, J. M., and J. M. Lynch (1983), Substrate flow and utilization in the rhizosphere of cereals, *New Phytol.*, 95(4), 605–623.
- Wieder, R. K. (2006), Primary production in boreal peatlands, in *Boreal Peatland Ecosystems*, *Ecol. Stud.*, vol. 188, edited by R. K. Wieder and D. H. Vitt, chap. 8, pp. 145–164, Springer, Berlin.
- Williams, T. G., and L. B. Flanagan (1996), Effect of changes in water content on photosynthesis, transpiration and discrimination against ^{13}C and $\text{C}^{18}\text{O}^{16}\text{O}$ in *Pleurozium* and *Sphagnum*, *Oecologia*, 108, 38–46.
- Williams, T. G., and L. B. Flanagan (1998), Measuring and modelling environmental influences on photosynthetic gas exchange in *Sphagnum* and *Pleurozium*, *Plant Cell Environ.*, 21, 555–564.
- Xu-Ri, , and I. C. Prentice (2008), Terrestrial nitrogen cycle simulation with a dynamic global vegetation model, *Global Change Biol.*, 14, 1745–1764.
- Yurova, A., A. Wolf, J. Sagerfors, and M. Nilsson (2007), Variations in net ecosystem exchange of carbon dioxide in a boreal mire: Modeling mechanisms linked to water table position, *J. Geophys. Res.*, 112, G02025, doi:10.1029/2006JG000342.
- Zobler, L. (1986), A world soil file for global climate modelling, *Tech. Memo. 87802*, 32, NASA.
-
- I. C. Prentice, QUEST, Department of Earth Sciences, University of Bristol, Wills Memorial Building, Queen's Road, Bristol BS8 1RJ, UK. (colin.prentice@bristol.ac.uk)
- I. Ross, Mathematics and Statistics, University of Victoria, P.O. Box 3060, STN CSC, Victoria, BC V8W 3R4, Canada. (ian@skybluetrades.net)
- R. Wania, School of Earth and Ocean Sciences, University of Victoria, Bob Wright Centre A405, P.O. Box 3065, STN CSC, Victoria, BC V8W 3V6, Canada. (rita@wania.net)